

**Supplemental information**

**Expanding the PRAAS spectrum: *De novo* mutations  
of immunoproteasome subunit  $\beta$ -type 10 in six  
infants with SCID-Omenn syndrome**

**Caspar I. van der Made, Simone Kersten, Odelia Chorin, Karin R. Engelhardt, Gayatri Ramakrishnan, Helen Griffin, Ina Schim van der Loeff, Hanka Venselaar, Annick Raas Rothschild, Meirav Segev, Janneke H.M. Schuurs-Hoeijmakers, Tuomo Mantere, Rick Essers, Masoud Zamani Esteki, Amir L. Avital, Peh Sun Loo, Annet Simons, Rolph Pfundt, Adilia Warris, Marieke M. Seyger, Frank L. van de Veerdonk, Mihai G. Netea, Mary A. Slatter, Terry Flood, Andrew R. Gennery, Amos J. Simon, Atar Lev, Shirley Frizinsky, Ortal Barel, Mirjam van der Burg, Raz Somech, Sophie Hambleton, Stefanie S.V. Henriët, and Alexander Hoischen**

## Supplemental Note: Case Reports

**Individual 1**, born to non-consanguineous parents, presented at 8-weeks of age with generalized erythroderma with desquamation and bullae, mild diarrhea, lymphadenopathy and failure to thrive (length and weight – 2.5 SD). Laboratory investigations at presentation showed T cells within normal range for age, but 4 days later the individual developed T cell lymphopenia. There was a predominantly memory CD4<sup>+</sup> CD45RO<sup>+</sup> T cell population and near absent naïve CD4<sup>+</sup> cells, cytotoxic CD8<sup>+</sup> cells and B-cells, with normal NK cell numbers, resulting in SCID with Omenn syndrome-like features. Maternofetal transfusion was excluded as XX-maternal T lymphocytes were absent. There was a markedly reduced lymphocyte proliferation following mitogen stimulation and defective IgG, IgA and IgM production. Skin biopsy at diagnosis showed hyperparakeratosis, pronounced apoptotic keratinocytes surrounded by lymphocytes, and flat epidermis with vacuolization of basal epidermal layer. At that time no genetic diagnosis could be made and individuals' fibroblasts had normal sensitivity to radiation. Before the age of 3 months, the individual received an allogeneic HSCT from his HLA identical brother. SCT was complicated by graft-versus-host disease (GVHD) of the skin and intestine. The individual's immune cell subsets normalized post-HSCT with reconstitution of the entire T-cell repertoire, and B and NK cells. Three years post-HSCT, he developed encephalopathy, quadriplegia, and neurogenic bladder due to cyclosporine toxicity. A year later, treatment was complicated by a Parvovirus B19 infection with myocarditis and dilated cardiomyopathy. Any immunosuppressive treatment was stopped with complete resolution of cardiac function. In follow-up he shows excellent vaccination responses and remains completely immunocompetent. He is an emotionally strong young adult, with normal intelligence. Physically, beyond the consequences related to the history of cyclosporine toxicity, he continues to have infection- and drug-induced cutaneous hypersensitivity which, histologically, could not be correlated to any graft versus host disease.

**Individual 2** was born following an uneventful pregnancy to healthy, non-consanguineous parents. He initially presented at two weeks following neonatal screening results of reduced TRECs (T-cell receptor excision circles) on Guthrie card. Physical examination was notable for thin sparse hair, a mild facial rash and mild dysmorphic facial features (protruding ears with pointed chin), adducted left thumb, hypospadias and micropenis. Initial testing showed a lack of T cells, with positive B cells on flow cytometry and a clonal T cell receptor repertoire. However, repeated testing revealed absent B cells in peripheral blood, and the phenotype was hence classified as a T-cell negative, B-cell negative and NK-cell positive SCID with an Omenn like phenotype. Treatment with preventive antibiotics and IVIG was commenced. At the age of one month the individual presented with CMV encephalitis and multisystem involvement, including seizures, and intractable diarrhea with consequent neurologic impairment manifesting as global developmental delay and multiple brain infarcts with diffuse brain atrophy. Over the next two years, he developed repeated CMV viremias, resistant to oral antiviral treatment. Additional

manifestations included pulmonary infections; intractable diarrhea, intermittently depending on total parenteral nutrition (TPN), hepatocellular and cholestatic liver failure with renal tubulopathy. Later on he presented with febrile episodes accompanied by marked leukocytosis suspected to be of auto-inflammatory origin responding to steroid treatment. Colonic biopsy revealed colitis with cryptitis and crypt abscesses with increased apoptotic debris and crypt attenuation with plasma cells (CD138 and CD38) within the lamina propria. CMV staining was negative. Skin biopsy revealed vacuolar interface dermatitis with eosinophils and pigment laden macrophages in the infiltrate. Although SCT was considered at an early stage, it was deferred to the age of 2.5 years at another institution by the family, and also due to his complex neurologic and CMV-related sequela. The individual died shortly after the procedure due to post transplant complications including transplant associated thrombotic microangiopathy (TMA).

**Individual 3** was born at full term to healthy unrelated parents weighing 2.98kg. He was briefly observed on the neonatal intensive care unit because of possible meconium aspiration. Having been discharged well, he developed progressive watery diarrhoea from 3 weeks of age accompanied by an evolving rash. By 5 weeks of age he was below his birth weight with ongoing profuse diarrhoea, oral candidiasis and a generalised peeling and scaling erythroderma. His blood picture revealed eosinophilia and lymphopenia affecting all subsets; naive T cells and B cells were absent with residual T cells showing reduced T cell receptor diversity and impaired mitogen responses. The diagnosis of Omenn syndrome was made after excluding maternofetal engraftment, and supportive care including parenteral nutrition was provided. He received an unrelated umbilical cord transplant after reduced intensity conditioning using fludarabine and melphalan with alemtuzumab serotherapy. The peri-transplant course was stormy with severe sinusoidal obstruction syndrome and acute graft versus host disease of the skin, managed conventionally. Full donor chimerism persisted and there was partial immune reconstitution with sub-normal lymphocyte numbers but present humoral immune responses and no excess of infections. Nutritional rehabilitation could not be achieved and the individual went on to manifest a lifelong enteropathy requiring gastrostomy feeding, as well as chronic liver disease that was attributed to his SOS, and mild learning difficulties. In mid-childhood, he developed a mesangiocapillary glomerulonephritis that was refractory to immunosuppression and rapidly progressed to acute renal failure. He nonetheless stabilised on haemodialysis and eventually came to renal transplant but rejected this and eventually died of sepsis.

**Individual 4** was born weighing 3.74kg after an uneventful pregnancy to healthy unrelated parents; two older half siblings were well. From 6 weeks of age, she developed severe seborrhoeic dermatitis that began on the scalp but spread to involve the entire body. She developed diarrhoea and oral candidiasis, both of which were persistent. By 3 months there was a superimposed vesicular rash that proved positive for VZV and she was admitted to hospital apparently septic. *Pneumocystis jirovecii* was subsequently

identified in bronchoalveolar lavage fluid. Immunological investigations were consistent with Omenn syndrome, showing absent B cells, normal NK cells and a very abnormal T cell compartment lacking naïve T cells and heavily skewed towards CD4 cells. Some IgM and IgA production were present. The individual was treated for her many infections and received myeloablative conditioning for a maternal haploidentical SCT as per contemporary practice. She tolerated this poorly, developing capillary leak syndrome with severe pneumonitis and subsequently GVHD of both skin and gut. Under immunosuppression she deteriorated neurologically despite ongoing antiviral therapy and sadly succumbed. Post mortem examination revealed VZV encephalitis.

**Individual 5** was born weighing 3.43kg to unrelated healthy parents after a normal pregnancy; an elder sister was well. He manifested diarrhoea and weight loss from birth, rapidly developing a metabolic acidosis. By one month of age he was still below his birth weight despite parenteral nutrition and had reached our SCID referral unit via district and regional paediatric centres. His ongoing diarrhoea proved positive for adenovirus which was also present in the blood, associated with transaminitis. His blood picture was that of a leaky SCID with present IgM production despite very low lymphocyte numbers in all compartments, low numbers of naïve T cells and poor PHA response despite high background T cell proliferation. A lymph node biopsy was grossly abnormal, with few lymphocytes and no mature follicles present. Within weeks he developed a maculopapular rash over the trunk, limbs and face consistent with Omenn syndrome. This individual received an unrelated donor cord transplant after reduced toxicity conditioning using treosulfan, fludarabine and alemtuzumab. He experienced considerable gut and skin toxicity which evolved into an inflammatory picture managed as acute GVHD. Although able to be discharged from hospital off parenteral nutrition, this individual had major problems sustaining his weight over the following years with waxing and waning enteropathy and skin rash. There was a partial response to immunosuppression and flaring of symptoms upon withdrawal, although not histologically typical of GVHD and associated with ongoing norovirus in stool. He did not sustain normal T cell numbers despite 100% donor chimerism, likely due to corticosteroid toxicity, and succumbed to sepsis aged 4 years.

**Individual 6** was born at 38 weeks gestation following an elective Caesarean section for breech presentation. This is the parents' first child and parents are healthy and unrelated. The pregnancy was complicated by gestational diabetes. He was born weighing 3.57kg and was well at birth. He was identified as having SCID following newborn screening (low TRECs on day 5) and confirmatory lymphocyte subsets (T cell lymphopenia and absent naïve T cells). There was no evidence of maternofoetal engraftment. He was breastfed prior to the result of his NBS being known and was gaining weight appropriately. He was screened for infection (negative for respiratory, faecal and blood viruses), started on antimicrobial prophylaxis (fluconazole, co-trimoxazole) and palivizumab, and had tissue typing in anticipation of receiving a HSCT. He also received respiratory syncytial virus prophylaxis

with palivizumab. Given his age and the NBS result he did not receive any vaccinations. Clinical exome sequencing followed by targeted analysis of known and candidate genes identified a variant in *PSMB10*. Capillary sequencing of patient and parental genomic DNA confirmed this to be *de novo* in origin. T cell proliferation was diminished in individual 6 compared to control in response to phytohaemagglutinin (PHA), phorbol myristate acetate (PMA) and CD3 stimulation. He had normal T cell receptor V $\beta$  chain usage, as assessed by flow cytometry. He was admitted for HSCT at 8 weeks of age and at this point was noted to have some blood and mucus mixed in with his stools. Individual 6 received a parental haploidentical TCR $\alpha\beta$ /CD19 depleted transplant after a conditioning regimen containing antithymocyte globulin (ATG), rituximab, treosulfan and fludarabine. He tolerated conditioning well with minimal gut toxicity (he did not require any parenteral nutrition) but developed a transient erythema multiforme-like skin rash two weeks after receiving his transplant (HSV, enterovirus, mycoplasma negative) which resolved after stopping tazocin and co-trimoxazole. He engrafted with 100% donor chimerism and was well until 1 month post-transplant, when he developed new unexplained vomiting rapidly (hours) followed by a significant neurological deterioration with reduced level of consciousness, increased tone and seizures. Urgent magnetic resonance imaging revealed T2 hyperintensity involving the white matter extending from the periorlandic region to the internal and external capsules, temporal lobes, thalami, lentiform nucleus and pons. Intracranial arteries were patent. Cerebrospinal fluid showed elevated protein (2.24g/L) but was paucicellular and free of pathogens by culture, PCR and metagenomic analysis; autoantibodies were also negative. Whilst covering for infection with meropenem and aciclovir, this episode was managed with high dose corticosteroids as well as full supportive care including respiratory support, anticonvulsants and muscle relaxants, with partial recovery. Individual 6 is currently approximately 2 months post HSCT and has been discharged from hospital on levetiracetam, clonidine, baclofen, diazepam and a weaning dose of steroid. He is now smiling, fixing and following again. A repeat MRI showed maturation and some improvement of the previously identified white matter changes.

## Supplemental Figures

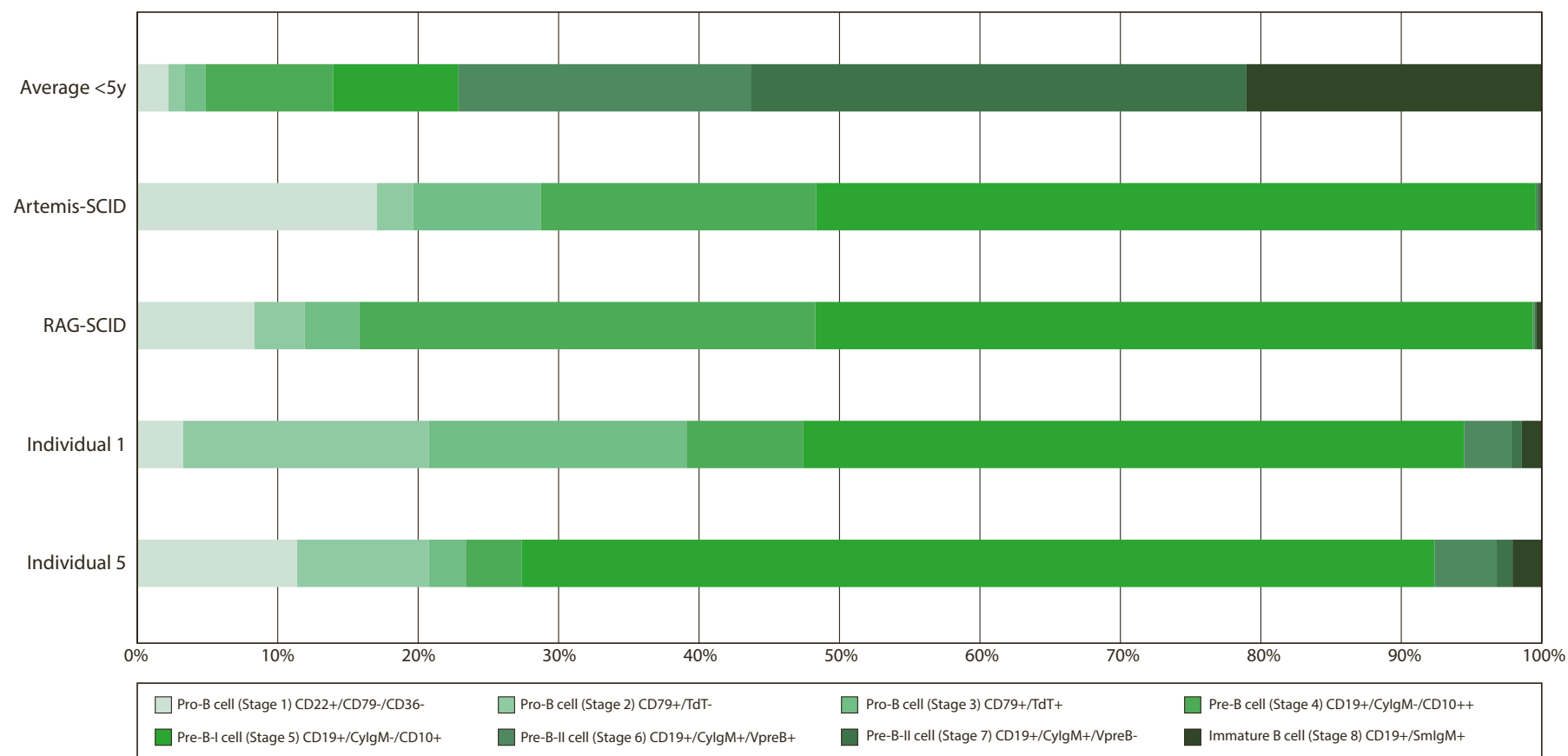


**Figure S1. Composition of bone marrow precursor B-cell compartment.**

B cell developmental stages were determined by flow cytometry on bone marrow biopsies obtained from individuals 1 and 5 and compared to healthy individuals <5y (n=9) and individuals with Omenn syndrome caused by Artemis deficiency (n=7) and RAG deficiency (n=17). All numbers are shown as percentages of the total measured B cells and have been corrected for blood contamination.

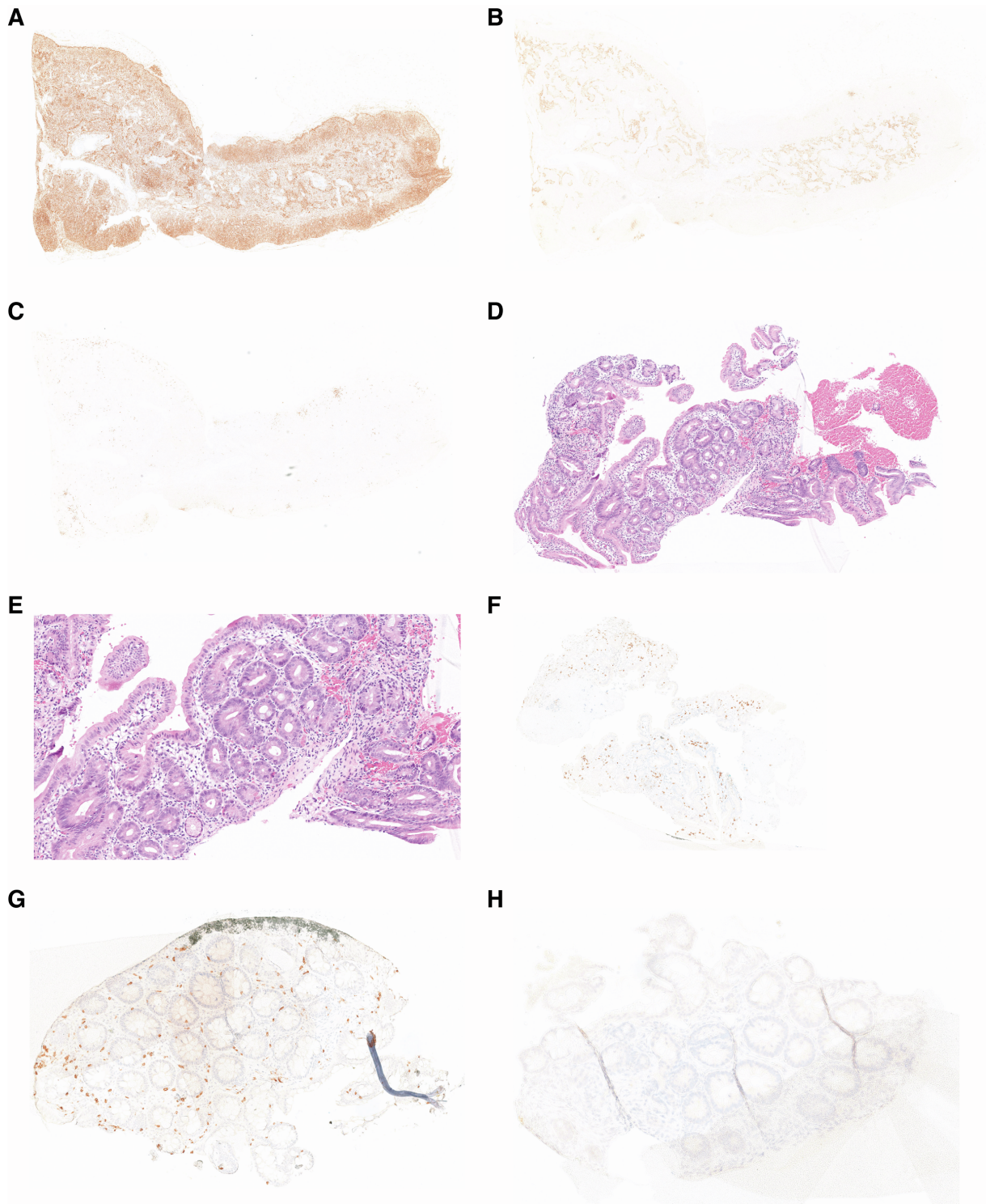


**Figure S2. Histopathological evaluation of tissue biopsies.**

(A-C) Immunohistochemistry of the inguinal lymph node from individual 5 showed a reduced number of T cells with a CD4+ majority (A) and small underlying CD21+ follicular dendritic cell meshworks (B) with sparse aggregates of CD79+ B-cells (C) associated with abortive primary follicle formation. There were no germinal centers. A small bowel biopsy from individual 5 showed focal villous atrophy (D) with increased mitosis and apoptotic bodies in the crypts (E) and reduced numbers of CD3+ T lymphocytes (F). Immunohistochemistry of the colon mucosa from individual 5 also indicated a reduced number of CD3+ T lymphocytes (G) and absent CD79+ plasma cells (H).

	<b>Individual 1</b>	<b>Individual 2</b>	<b>Individual 3</b>	<b>Individual 4</b>	<b>Individual 5</b>	<b>Individual 6</b>
<b>Ancestry</b>	European	Jewish Sephardi	European	European	European	European
<b>Mutation</b>	c.601G>A; p.Gly201Arg	c.601G>A; p.Gly201Arg	c.601G>C; p.Gly201Arg	c.601G>A; p.Gly201Arg	c.166G>C; p.Asp56His	c.166G>C; p.Asp56His
<b>Allele frequency<sup>a</sup></b>	0	0	0	0	0	0
<b>CADD score</b>	35	35	34	35	28	35
<b>Age at investigation (w)</b>	8	2	6	13	4	0
<b>Sex</b>	M	M	M	F	M	M
<b>Clinical presentation</b>	SCID/Omenn syndrome FTT, mild diarrhoea, skin rash, oral thrush, lymphadenopathy	SCID/Omenn FTT, severe diarrhoea, skin rash, intermittend TPN-dependent, hepatocellular and cholestatic liver failure with renal tubulopathy	SCID/Omenn syndrome FTT, diarrhoea, skin rash, oral thrush	SCID/Omenn syndrome FTT, skin rash, vesicular rash, oral thrush	SCID/Omenn syndrome FTT, severe diarrhoea, skin rash, disseminated adenovirus, TPN-dependent with elevated ALT	Newborn screening
<b>Rash</b>	Generalised erythroderma with desquamation and bullae.	Mild facial rash evolving into an erythematous papular rash with hyperpigmented macules	Generalised erythroderma with peeling	Thickened red skin with super-imposed crusting vesicular rash (VZV+)	Raised maculopapular rash on trunk, limbs and face, managed as OS with topical corticosteroid	Slightly rough erythematous rash to abdomen and chest
<b>Age at onset of rash (w)</b>	< 1	2	3	1	8	<1
<b>Alopecia (hair loss)</b>	Loss of hair between birth and clinical presentation with progression to total alopecia	Sparse hair	Sparse hair	Sparse hair	-	-
<b>Hepatomegaly</b>	-	-	1cm	2cm	-	-
<b>Infection and inflammation</b>	Oral candidiasis, secondary skin infection (S. aureus) Otitis media	CMV encephalitis and multi-organ involvement (4w of age), multiple episodes of respiratory insufficiency	Oral candidiasis Septic episode pre-transplant	Oral candidiasis Chronic VZV PCP on BAL Ear discharge (otitis media?)	Disseminated adenovirus	-



		requiring prolonged mechanical ventilation. Recurrent episode of systemic inflammation responsive to steroids				
<b>Dysmorphology</b>	Overfolded helices, hypoplasia alae nasi, cone-shaped teeth, hypodontia	Mild dysmorphic facial features (protruding ears with pointed chin), adducted left thumb, hypospadias and micropenis. Dysplastic nails.	No	No	No	No

**Table S1. Extended genetic and clinical information.**

<sup>a</sup> Allele frequency in GnomAD, dbSNP or ExAC databases.

ALT, alanine aminotransferase; BAL, broncho-alveolar lavage; CADD, combined annotation dependent depletion; CMV, cytomegalovirus; FTT, failure to thrive; OS, Omenn Syndrome; PCP, pneumonia due to *Pneumocystis jirovecii*; SCID, severe combined immunodeficiency; TPN, total-parenteral nutrition; VZV, varicella zoster virus

	Individual 1	Individual 2	Individual 3	Individual 4	Individual 5	Individual 6
<b>Age at investigation (w)</b>	8	2	6	12	4	2
<b>Eosinophils (/µl) (40-800)</b>	896	2930	1700	1700	720	1000
<b>IgG (g/L) (3.7-12.6)</b>	1.35	0.974	2.6	2.76	5.1	2.4
<b>IgA (g/L) (0.02-0.15)</b>	< 0.07	< 0.01	<0.07	0.23	0.41	<0.04
<b>IgM (g/L) (0.05-0.29)</b>	< 0.07	< 0.02	0.09	0.12	0.98	<0.04
<b>CD3 (/µl) (1700-3600)</b>	1300	1552	595	1239	188	309
<b>CD4 (/µl) (1700-2800)</b>	1100	730	551	1143	137	272
<b>CD8 (/µl) (800-1200)</b>	40	820	72	83	26	60
<b>CD4:CD8 ratio</b>	27.5	0.89	7.7	13.8	5.3	4.5
<b>CD19 (/µl) (500-1500) (%)</b>	40	430 (disappeared shortly after presentation)	0	<1	19	34
<b>CD16/CD56 (/µl) (300-700)</b>	70	1826	46	414	22	368
<b>CD45RA (%CD3)</b>	8.6	NA <sup>a</sup>	NA	0	8 (CD45RA+CD27+)	0
<b>CD45RO (%CD3)</b>	95	NA <sup>a</sup>	91	NA	NA	4
<b>TCR αβ (%CD3)</b>	98	NA	97	99	74	96
<b>TCR γδ (%CD3)</b>	2	NA	3	1	26	4
<b>PHA stimulation index (control)</b>	PHA 10900 cpm (ref. > = 17000)	Limited TCR repertoire with decreased mitogen response	10 (415)	3 (238)	10 (418)	31
<b>PHA counts individual (control)</b>	NA	NA	16558 (85097) <sup>c</sup>	NA	52976 <sup>c</sup> (69434)	130
<b>Skin (biopsy)</b>	Hyperparakeratosis, pronounced apoptotic keratinocytes surrounded by lymphocytes, flat epidermis with vacuolization of basal epidermal layer <sup>b</sup>	Vacuolar interface dermatitis with eosinophils and pigment laden macrophages in the infiltrate	Flattened epidermis with widespread basal vacuolation. Eosinophilic keratinocytes with pyknotic nuclei are seen within the epidermis, some associated with adjacent lymphocytes – the features of satellite cell necrosis. The superficial dermis contains a moderate perivascular chronic inflammatory cell infiltrate. The features are those of lichenoid inflammation and essentially identical to GVHD grade 2	NA	NA	NA
<b>Lymph node (biopsy)</b>	-	-	-	-	Paucicellular, stroma-rich	-

					lymph node with moderate numbers of interdigitating dendritic cells/Langerhans cells and eosinophils, but the nodular and diffuse “dermatopathic” changes characteristically seen in OS are not present. The vast majority of T cells present are CD4+ cells. Occasional large CD30+ cells, most likely activated T cells, are present. The few B cells associated with FDC meshworks are shown to be IgD+, consistent with abortive primary follicles.	
<b>Bone marrow (aspirate)</b>	Block in B cell maturation	-	-	-	Block in B cell maturation	-
<b>Gastrointestinal tract (endoscopy, biopsy)</b>	-	Colonic biopsy: colitis with cryptitis and crypt abscesses with increased apoptotic debris and crypt attenuation with plasma cells (CD138 and CD38) within the lamina propria.	Upper GI endoscopy and biopsy: Partial villous atrophy. Nodular macroscopic appearance of jejunum. CD3-CD4+ cells present; no T cells.	-	Pre-transplant GI endoscopy: consistent with immunodeficiency related enteropathy	-
<b>Other</b>	In the skin biopsy before HSCT two clonal TCRG gene rearrangements were detected, indicating the presence of a biallelic rearranged clonal T-cell population (*)	TCR Vb repertoire analysis showed clonal expansions of two VbR's: Vb3, Vb) and lack of most other VbR's, suggestive of autoreactive clonal expansion as seen in individuals with SCID and OS.	TCR Vb usage: 73% of CD3 pos cells were pos for TCRVB families tested with increase in TCRVB2 and TCRVB14 and absent TCRVB11, 16, 18, 23 and 24 families. Clonal TCR rearrangements detected (TCRVBJA, VBJB, TCRVGJB and TCRD)	NA	NA	Normal Vb usage (CD3+CD4+ and CD3+CD4-)

**Table S2. Extended laboratory and histopathological information.**

Laboratory parameters are presented with units and normal reference ranges if applicable.

<sup>a</sup> For this individual TREC copies were available with significantly reduced levels (179 with reduction to 5 over time).

<sup>b</sup> Previously published in D'Hauw et al. British Journal of Dermatology 2008<sup>1</sup>.

<sup>c</sup> High background in individual

FDC, follicular dendritic cell; GVHD, graft-versus-host-disease; NA, not assessed; OS, Omenn Syndrome; PHA, phytohaemagglutinin; SCID, severe combined immunodeficiency; TCR, T cell receptor;

	<b>Individual 1</b>	<b>Individual 2</b>	<b>Individual 3</b>	<b>Individual 4</b>	<b>Individual 5</b>	<b>Individual 6</b>
<b>Age at transplantation (w)</b>	12	130	11	16	12	8
<b>Materno-fetal engraftment</b>	EXCLUDED by X-Y FISH and microsatellite markers	-	EXCLUDED by X-Y FISH and microsatellite markers	-	-	Excluded by microsatellite markers
<b>Donor information</b>	10/10 HLA identical sibling	ATG	URD	Maternal haplo	9/10 mM cord blood	Paternal haplo
<b>Serotherapy</b>	ATG 5 mg/kg	Cyclosporine + MMF	alemtuzumab	ATG 6 mg/kg	None	ATG 5mg/kg, Rituximab 20mg/m <sup>2</sup>
<b>Chemotherapy</b>	CsA	Engraftment failure, pancytopenia	Flu mel	Bu 4 mg/kg, cyclo 200 mg/kg	Treo 36 g/m <sup>2</sup> , Flu 150 mg/m <sup>2</sup>	Treo 10g/m <sup>2</sup> , Flu 40mg/m <sup>2</sup>
<b>Outcome</b>	100% donor	ATG	100% donor	-	100% donor	-
<b>Post-HSCT complications</b>	Severe skin and gut GvHD	Post-transplant complications incl. transplant associated TMA, sepsis with multi-organ failure	Skin GVHD Severe VOD	Pneumonitis with capillary leak peri-engraftment GVHD skin and gut Hypertension Recurrence of VZV with fatal encephalopathy	Skin GVHD with late recurrence (12m), steroid-sensitive Marked mucositis and skin toxicity Adeno-viraemia Liver dysfunction with marked ductular cholestasis on biopsy	Acute leuko-encephalopathy
<b>Follow-up</b>	Alive, 18 yrs post HSCT Encephalopathy, quadriplegia and neurogenic bladder due to CsA toxicity Parvovirus B19 Myocarditis Osteoporosis Kerato-	Died post-HSCT (131 weeks)	Died age 16 yrs Long term enteropathy Liver cirrhosis with varices Mesangiocapillary GN with acute renal failure, ESRD requiring dialysis (and rejected renal allograft)	Died post-HSCT (11w)	Died age 4 yrs Sudden profound hypothyroidism Long term enteropathy FTT with norovirus infections, managed with immune-suppression, flares during	Alive, 2m post-HSCT

	conjunctivitis sicca Marked sensitive and hyper-responsive skin in response to infections and certain drugs		Learning difficulties		tapering, died due to recurrent infections	
--	--	--	-----------------------	--	--	--

**Table S3. Extended information on hematopoietic stem cell transplantation therapy**

ATG, antithymocyte globulin; Bu, busulfan; CsA, cyclosporin; Cyclo, cyclophosphamide; ESRD, end-stage renal disease; Flu, fludarabine; FTT, failure to thrive; GN, glomerulonephritis; GVHD, graft-versus-host-disease; Mel, melphalan; MMF, mycophenolate mofetil; TMA, thrombotic microangiopathy; Treo, treosulfan; VOD, veno-occlusive disease; VZV, varicella zoster virus

	Individual 1	Individual 2	Individual 3	Individual 4	Individual 5	Individual 6
Candidate variants within the IEI panel	<i>FLG</i> (Chr1:g.152285 861G>A NM_002016: c.1501C>T, p.(Arg501Ter))	-	-	-	<i>TNFSF12</i> (Chr17:746063 3T>C NM_003809.3: c.716T>C, p.(Phe239Ser)	- <sup>a</sup>
Possible <i>de novo</i> variants (if trio analysis was performed)	<i>PSMB10</i> (Chr16:g.67968 809C>T; NM_002801: c.601G>A p.(Gly201Arg))	<i>PSMB10</i> (Chr16:g.67968 809C>T; NM_002801: c.601G>A p.(Gly201Arg))	-	-	-	<i>PSMB10</i> (Chr16:g.67968 809C>T; NM_002801: c.601G>A p.(Gly201Arg)) on prospective screening
	<i>CCNE1</i> (Chr19:g.30314 571C>T; NM_001238.4: c.1120C>T, p.(Arg374Ter))	<i>SLC30A5</i> (Chr5:g.684132 08G>A; NM_022902: c.1424G>A, p.Arg475Gln)	-	-	-	-

**Table S4. Candidate variants remaining after WES filtering**

<sup>a</sup> None within NHS Genomics England Panel for Primary immunodeficiency or monogenic inflammatory bowel disease (V4.0) (<https://panelapp.genomicsengland.co.uk/panels/398>)

## Subjects & methods

### Study participants and ethics approval

Individual 1 was referred to the Department of Pediatrics at the Radboud University Medical Center at 8 weeks of age. Individual 2 presented to the Pediatric Immunology Unit at the Sheba Medical Center after abnormal newborn screening raising suspicion of severe combined immunodeficiency (SCID). Written informed consent and publication consent were obtained from individuals and/or their parents and were approved by the local Ethics Committees. Individuals 3-6 were referred to the Paediatric Immunology and haematopoietic stem cell transplantation (HSCT) team at the Great North Children's Hospital (or its predecessor, Newcastle General Hospital) in Newcastle upon Tyne. Their parents provided generic consent for future research through ethically approved procedures (REC reference 10/H0906/22 or 20/NE/0044).

### Whole-exome sequencing analysis

Clinical whole-exome sequencing was performed on genomic DNA extracted from whole blood of individuals 1-2 and their parents according to standard hospital procedures. Individuals 3-5 underwent whole exome sequencing retrospectively and as singletons using dermal fibroblast (individuals 3 and 4) or whole blood (individual 5) genomic DNA as a research procedure. Coding regions were enriched using the *SureSelect Human All Exon V5 Kit (Agilent, Santa Clara, United States)* and sequenced on the Illumina HiSeq platform (HiSeq 4000 for individual 1, HiSeq 2500 for individuals 2-5; Illumina Inc., San Diego, CA, United States; AROS (Applied Biotechnology AS, Denmark)). Sequence reads were aligned to the human reference genome (hg19) with the Burrows-Wheeler Aligner Algorithm and variants were called using the HaploTypeCaller algorithm of GATK. For all individuals, in-house custom analysis pipelines were applied for variant annotation.<sup>2</sup> KGG-seq v.08 was used for annotation of identified variants in individual 2. Variants were first prioritized in a diagnostic setting by filtering for coding, nonsynonymous variants with allele frequencies below 1% in the in-house database or population databases (dbSNP ExAC and GnomAD) in genes included in the *in silico* gene panel for inborn errors of immunity. Subsequently, downstream filtering was performed to retain rare variants (MAF <0.1%) variants with a minimum of 5 variant reads and >20% variation and *de novo* status using the DeNovoCheck tool (**Table S4**). More technical details for individual 1 can be retrieved from a previously published series of individual-parent exome trio sequencing for inborn errors of immunity, that included this individual.<sup>3</sup> Moreover, nucleotide conservation (PhyloP<sup>4</sup>) and *in silico* pathogenicity predictors, *i.e.* PolyPhen2,<sup>5</sup> SIFT,<sup>6</sup> Mutation Taster,<sup>7</sup> PROVEAN,<sup>8</sup> Mutation Assessor<sup>9</sup> and CADD\_Phred<sup>10</sup> were used for variant prioritization. Individual 6 was identified following newborn screening as having low TRECs. Subsequent clinical whole exome sequencing was negative against NHS England's primary immunodeficiency gene panel (R15) but targeted research analysis identified a variant in *PSMB10*.

### **Genome-wide SNP array**

SNP-array analysis was performed in individual 1 to identify copy-number variants and regions of altered B-allele frequency including regions of (somatic) homozygosity as described previously.<sup>11</sup> Chromosomal SNP-based microarray was conducted for individual 2 on a Baylor medical genetics laboratories targeted postnatal oligo v8.1.1 platform, returning a normal result.

### **Sanger and amplicon sequencing**

The *de novo* status of the identified *PSMB10* variants was determined in trio-WES data (Individuals 1 and 2) or assessed by standard Sanger sequencing (Individuals 3-6). All available parental samples (11 of 12) were wild type. In individual 1, deep amplicon sequencing was performed as previously described,<sup>12</sup> enabling accurate identification of the variant allele fractions (VAF) across the two different tissue samples.

### **Somatic UPD/RM calling in exome data**

To estimate the level of mosaicism, *i.e.* proportion of abnormal cells with (segmental) chromosomal abnormalities, as well as their parental origin, we applied haplarithmisis<sup>13</sup> as previously described<sup>14</sup> with some modifications to adapt our approach for WES. Briefly, we applied haplotypcaller from the GATK tool haplotypcaller<sup>15</sup> to determine SNVs annotated in the dbSNP database (version 150). Subsequently, using the R-function `extract.gt` (`vcfR` package bioconductor), depth of coverage of each genomic location was calculated per sample and BAF values were determined. We then applied trio analysis option of haplarithmisis for determining parental haplarithms, and QDNAseq for determining logR-values per 10kb bins.<sup>16</sup> We then estimated the level of mosaicism by calculating the distortion of segmented haplarithm values from the expected 1:1 allelic ratio, *i.e.*, 0.5:0.5 vertical distance in each segmented parental haplarithms.

### **Structural modelling**

The structural impact of the p.(Asp56His) and p.(Gly201Arg) variants in *PSMB10* were modelled using experimentally determined 3D structures of the 20S proteasome (PDB: 6E5B), as well as its 26S proteasome homologue (PDB: 6MSB). Variants in the TUB6 mouse model, p.(Gly170Trp) and the p.(Gly201Arg) equivalent, were modelled into the crystal structure of mouse 20S proteasome (PDB: 3UNH). Changes in protein stabilities upon mutations were estimated using FoldX energy function (v.5.0).<sup>17</sup> For a given mutation, structural models were constructed using RepairPDB and BuildModel functions with 5 iterations of sidechain rotamer adjustments, followed by calculation of average of the differences in free energies between wildtype and the mutant structures in kcal/mol.

### **Immunoblotting**



Primary dermal fibroblasts at low passage number were seeded at 100,000 per well of 6-well plate and treated, or not, with interferon-gamma at 200 IU/ml (Immunikin, Boehringer Ingelheim, Germany) for 48 hrs. Each well was washed with PBS and lysed using radio-immunoprecipitation assay buffer (RIPA; 150mM sodium chloride, 1% Triton X-100, 0.5% sodium deoxycholate, 0.1% sodium dodecyl sulphate, 50mM Tris pH7.4) supplemented with cOmplete™ Protease Inhibitor Cocktail and PhosSTOP™ Phosphatase inhibitor Cocktail (Roche, Switzerland). Lysates were denatured at 70°C for 15 minutes with 10% dithiothreitol (DTT), and 1X NuPAGE LDS Sample Buffer (Thermo Fisher Scientific, USA) then loaded on to 4-12% Bis-Tris gel alongside pre-stained protein ladder (PageRuler Plus, Thermo Fisher Scientific, USA) for gel electrophoresis in 1X NuPAGE MOPS SDS Running Buffer (Invitrogen, USA). An equal volume of lysate was loaded per lane. Proteins were transferred to 0.45mM polyvinyl difluoride (PVDF) membranes (Millipore, USA) at 20V using 1X NuPAGE Transfer Buffer (Invitrogen, USA) in 20% methanol. Membranes were blocked for 60 minutes using 5% bovine serum albumin in tris-buffered saline with 0.1% Tween (TBS-T) prior to immunostaining. Membranes were incubated overnight with anti-PSMB10 and anti-alpha-Tubulin primary antibodies (PSMB10/MECL-1 (E6R7O) Rabbit mAb #17579 (final concentration: 1:1000) and alpha-Tubulin (DM1A) mouse mAb #3873 (final concentration 1:10,000) from Cell Signaling Technology) followed by washing and incubation with anti-rabbit-IgG-HRP and anti-mouse-IgG-HRP secondary antibodies (final concentrations: 1:5000; #7074S and #7076S respectively, Cell Signaling Technology). Membranes were developed with Immobilon ECL substrate (Millipore, USA) and chemiluminescent images were visualized with the LI-COR Odyssey (LI-COR, USA).

## Supplemental references

1. D'hauw, A., Seyger, M.M.B., Groenen, P.J.T.A., Weemaes, C.M.R., Warris, A., and Blokk, W.A.M. (2008). Cutaneous graft-versus-host-like histology in childhood. Importance of clonality analysis in differential diagnosis. A case report. *Br J Dermatol* 158, 1153–1156. 10.1111/j.1365-2133.2008.08497.x.
2. De Ligt, J., Willemsen, M.H., Van Bon, B.W.M., Kleefstra, T., Yntema, H.G., Kroes, T., Vulto-van Silfhout, A.T., Koolen, D.A., De Vries, P., Gilissen, C., et al. (2012). Diagnostic Exome Sequencing in Persons with Severe Intellectual Disability. *N Engl J Med* 367, 1921–1929. 10.1056/NEJMoa1206524.
3. Hebert, A., Simons, A., Schuurs-Hoeijmakers, J.H., Koenen, H.J., Zonneveld-Huijssoon, E., Henriët, S.S., Schatorjé, E.J., Hoppenreijts, E.P., Leenders, E.K., Janssen, E.J., et al. (2022). Trio-based whole exome sequencing in patients with suspected sporadic inborn errors of immunity: a retrospective cohort study. *eLife*. 10.7554/eLife.78469.
4. Pollard, K.S., Hubisz, M.J., Rosenbloom, K.R., and Siepel, A. (2010). Detection of nonneutral substitution rates on mammalian phylogenies. *Genome Res.* 20, 110–121. 10.1101/gr.097857.109.
5. Adzhubei, I.A., Schmidt, S., Peshkin, L., Ramensky, V.E., Gerasimova, A., Bork, P., Kondrashov, A.S., and Sunyaev, S.R. (2010). A method and server for predicting damaging missense mutations. *Nat Methods* 7, 248–249. 10.1038/nmeth0410-248.
6. Vaser, R., Adusumalli, S., Leng, S.N., Sikic, M., and Ng, P.C. (2016). SIFT missense predictions for genomes. *Nat Protoc* 11, 1–9. 10.1038/nprot.2015.123.
7. Schwarz, J.M., Cooper, D.N., Schuelke, M., and Seelow, D. (2014). MutationTaster2: mutation prediction for the deep-sequencing age. *Nat Methods* 11, 361–362. 10.1038/nmeth.2890.
8. Choi, Y., Sims, G.E., Murphy, S., Miller, J.R., and Chan, A.P. (2012). Predicting the Functional Effect of Amino Acid Substitutions and Indels. *PLoS ONE* 7, e46688. 10.1371/journal.pone.0046688.
9. Reva, B., Antipin, Y., and Sander, C. (2011). Predicting the functional impact of protein mutations: application to cancer genomics. *Nucleic Acids Research* 39, e118. 10.1093/nar/gkr407.
10. Rentzsch, P., Witten, D., Cooper, G.M., Shendure, J., and Kircher, M. (2019). CADD: predicting the deleteriousness of variants throughout the human genome. *Nucleic Acids Research* 47, D886–D894. 10.1093/nar/gky1016.
11. Jongmans, M.C.J., Verwiel, E.T.P., Heijdra, Y., Vulliamy, T., Kamping, E.J., Hehir-Kwa, J.Y., Bongers, E.M.H.F., Pfundt, R., van Emst, L., van Leeuwen, F.N., et al. (2012). Revertant Somatic Mosaicism by Mitotic Recombination in Dyskeratosis Congenita. *The American Journal of Human Genetics* 90, 426–433. 10.1016/j.ajhg.2012.01.004.
12. Acuna-Hidalgo, R., Sengul, H., Steehouwer, M., Vorst, M. van de, Vermeulen, S.H., Kiemeny, L.A.L.M., Veltman, J.A., Gilissen, C., and Hoischen, A. (2017). Ultra-sensitive Sequencing Identifies High Prevalence of Clonal Hematopoiesis-Associated Mutations throughout Adult Life. *The American Journal of Human Genetics* 101, 50–64. 10.1016/j.ajhg.2017.05.013.
13. Zamani Esteki, M., Dimitriadou, E., Mateiu, L., Melotte, C., Van der Aa, N., Kumar, P., Das, R., Theunis, K., Cheng, J., Legius, E., et al. (2015). Concurrent Whole-Genome Haplotyping and Copy-Number Profiling of Single Cells. *The American Journal of Human Genetics* 96, 894–912. 10.1016/j.ajhg.2015.04.011.
14. Zamani Esteki, M., Viltrop, T., Tšuiiko, O., Tiirats, A., Koel, M., Nõukas, M., Žilina, O., Teearu, K., Marjonen, H., Kahila, H., et al. (2019). In vitro fertilization does not increase the incidence of de novo copy number alterations in fetal and placental lineages. *Nat Med* 25, 1699–1705. 10.1038/s41591-019-0620-2.
15. McKenna, A., Hanna, M., Banks, E., Sivachenko, A., Cibulskis, K., Kernytsky, A., Garimella, K., Altshuler, D., Gabriel, S., Daly, M., et al. (2010). The Genome Analysis Toolkit: A MapReduce framework for analyzing next-generation DNA sequencing data. *Genome Res.* 20, 1297–1303. 10.1101/gr.107524.110.
16. Scheinin, I., Sie, D., Bengtsson, H., Van De Wiel, M.A., Olshen, A.B., Van Thuijl, H.F., Van Essen, H.F., Eijk, P.P., Rustenburg, F., Meijer, G.A., et al. (2014). DNA copy number analysis of fresh and formalin-fixed specimens by shallow whole-genome sequencing with identification and

exclusion of problematic regions in the genome assembly. *Genome Res.* 24, 2022–2032. 10.1101/gr.175141.114.

17. Schymkowitz, J., Borg, J., Stricher, F., Nys, R., Rousseau, F., and Serrano, L. (2005). The FoldX web server: an online force field. *Nucleic Acids Research* 33, W382–W388. 10.1093/nar/gki387.